XIII_1856

Physica Macedonica **61**, (2012) p. 27-38

ISSN 1409-7168

IMPEDANCE SPECTROSCOPY ANALYSIS OF $YCrO_3$ AND $YCo_{0.5}Cr_{0.5}O_3$

M. Pecovska Gjorgjevich[1], S. Aleksovska[2] and S. Dimitrovska-Lazova[2]

[1]Institute of Physics, Faculty of Natural Sciences and Mathematics,

[2]Institute of Chemistry, Faculty of Natural Sciences and Mathematics,

"Sts Cyril and Methodius" University, 1000 Skopje, R Macedonia

Abstract. $YCrO_3$ and $YCo_{0.5}Cr_{0.5}O_3$ were prepared by solution combustion method and additionally heated at 800^0C for 4 hours. The X-ray diffraction analysis showed an orthorhombic phase of perovskite structure. The electrical properties of the pellets are investigated by impedance spectroscopy in the temperature range 301-339 K and frequency range 10Hz to 10MHz (bellow dielectric phase transition temperature ~ 400 K). Impedance measurements show increase of *Z'* and *Z"* with temperature, which indicates that dc conductivity decreases with heating (metallic behavior). The Nyquist plot reveals non-Debye behavior with possible two relaxation process for $YCrO_3$ and $YCoCrO_3$. The relaxation times of processes involved were calculated. The most probable relaxation times follow the Arrhenius law which allows us to estimate the activation energies of the processes in the perovskite materials. AC conductivity slope shows two processes, one starting from ~1MHz for all temperatures and another initiating from 325 K in the medium frequency range. The start of the conductivity dispersion is moving towards lower frequencies with increasing temperature. Activation energy of dc conductivity is calculated. The ac conductivity behavior is analyzed using Jonscher's power law $\sigma = A\omega^n$. The influence of Co in the structure is observed in an increasing conductivity and change in the conductivity process for higher temperatures.

PACS: 77.84.-s, 72.80.-r, 84.37.+q

1. INTRODUCTION

The perovskite-like structure, named after the CaTiO3 perovskite mineral,[1] is a ternary compound of formula ABO_3 where A and B cations differ in size. Perovskite structure materials play an important role in dielectric ceramics with different effects on physical properties because of variation of ionic size and small displacements of atoms which lead to the distortion of the structure and the reduction of symmetry.

The rare-earth chromate $YCrO_3$ is a perovskite like ceramic which exhibits weak ferromagnetism below T_N = 140 K (canted antiferromagnetic order), and is also a weak ferroelectric below T_C = 470 K, (weak polarization and dielectric anomaly appear).[2] This type of materials are called biferoics (multifunctional materials which are both ferromagnetic and ferroelectric) and are very interesting because of their potential application in technology as

high-temperature electrode and thermoelectric materials. In such materials the impedance and dielectric properties are of great scientific and technological interest.

ABO_3 perovskite ceramics exhibit relatively high electrical conductivity at elevated temperatures by substitution on either the A or B sites with acceptor- or donor-type cations. The factors that define their dielectric behavior are intrinsic (crystal structure, phonon interaction etc) and extrinsic (heterogenity of the medium such as porosity, impurities, grain boundaries and random crystal orientation.[3] The electrical conductivity in $YCrO_3$ is essentially due to the 3rd band of the Cr ions.[4] The modification in B ion (replacement of Cr with Co) also modify the dielectric response characteristics. $YCo_{0,5}Cr_{0,5}O_3$ is also a perovskite that shows biferoic behavior with some differences in the structure and therefore in the electric behavior. As we know ferroelectricity requires the displacement of the B cation in the ABO_3 structure (A and B are cations and O is anion) relative to the oxygen cage to create an electric dipole moment.

In this article we will observe impedance and conductivity changes of these two types of perovskites owing to frequency and temperature variations. Complex Impedance Spectroscopy (CIS) is a well known and powerful technique used for analysis of the electrical properties of electroceramics. It involves measurements of real and imaginary parts of impedance for a wide range of frequency and enables one to resolve the contributions of various processes such as grain effects, grain boundary and electrode polarization and activation energy of the processes involved. Complex data can be represented in any of the four related basic formalisms: complex impedance Z*, complex permittivity ε*, complex admittance Y* and complex modulus M*. Since relaxation times of processes involved are different because of different capacitive components, we use complex impedance plot (Nyquist plot) to define one, two or three semicircular arcs corresponding to high frequency end bulk electrical conduction, intermediate frequency range connected to conduction by grain boundaries and low frequency arc from electrode processes. Each of these semicircles could be represented by a single *RC* combination connected to the relaxation time of the process ($\tau = RC$), where *R* is the ohmic resistance and *C* is the capacitance of the certain circuit. The depressed semicircle with center below the real axis gives non-Debye behavior indicating the presence of CPE (distributed element). The semicircle passes through a maximum at angular frequency ω (relaxation frequency) and satisfies the condition $\omega\tau = 1$.

2. THEORY AND DISCUSION

The classical model to describe the impedance behavior is that of Debye and it is written in the form:

$$Z^* = Z' - iZ'' = \frac{R}{1 + i\omega\tau}, \tag{1}$$

where $\tau = RC$. This equation implies a simple RC circuit in parallel which gives rise to a semicircle whose center lies on the real axis in the complex plane (Z'' vs. Z') or a Debye peak in the spectroscopic plots of the imaginary component (Z' vs. log f) where:

$$Z' = \frac{R}{1+(i\omega RC)^2} \tag{2}$$

and

$$Z'' = R\frac{\omega RC}{1+(i\omega RC)^2}. \tag{3}$$

In the above equations ω is the angular frequency. Usually the center of the semicircle lies off the real axis by an angle θ (= $\beta\pi/2$). It is described by the following equation:

$$Z^* = \frac{R}{1+(i\omega RC)^n}, \tag{4}$$

$n = 1 - \beta$, where β is the angle of deviation from the ideal semicircular arc. The simple Debye equation for the relaxation is the case for $\beta = 0$, i.e., $n = 1$. Complex impedance plane plots of Z' versus Z'' (where Z' and Z'' are the real and imaginary parts of the complex impedance plane, respectively) are useful for determining the dominant resistance of a sample but are insensitive to the smaller values of resistances.

In the present investigation, we used Impedance Spectroscopy for analyzing $YCrO_3$ and $YCo_{0.5}Cr_{0.5}O_3$ perovskite structures in temperature range 301-339 K and frequency range 10 Hz - 10 MHz. The perovskites $YCrO_3$ and $YCo_{0.5}Cr_{0.5}O_3$ were prepared by solution combustion method using urea as a fuel and additionally heated at 800^0C for 4 hours. The X-ray difraction analysis of the crystal structures showed that both compounds crystallize in the orthorhombic space group *Pnma* with four formula units per unit cell.

Table1. The lattice cell parameters, relative atomic coordinates, temperature factors and R-factors.in the structure of $YCrO_3$ and $YCo_{0,5}Cr_{0,5}O_3$

Атоми	Парам.	$YCo_{0,5}Cr_{0,5}O_3$	$YCrO_3$
	a (Å) *b* (Å) *c* (Å)	5,4725(3) 7,4524(4) 5,1926(2)	5,5210(2) 7,5317(3) 5,2404(2)
Y	*x* *z* *B*	0,06691(15) 0,9839(3)	0,0660(26) 0,9826(5) 1,79(5)
O1	*x* *z* *B*	0,4708(10) 0,0993(9)	0,4637(17) 0,1104(18) 1,9(3)
O2	*x* *y* *z* *B*	0,3007(8) 0,0534(5) 0,6966(8)	0,2981(15) 0,0537(10) 0,6936(14) 2,0(2)
R_I	R_p: R_{wp}: R_{exp}: χ^2:	12,1 8,97 2,66 11,3	16,9 14,9 12,2 1,49

Table2. Selected distances and angles in the structure of $YCrO_3$ and $YCo_{0,5}Cr_{0,5}O_3$.

	$YCo_{0,5}Cr_{0,5}O_3$	$YCrO_3$
Y−O1	3,317	3,3912
	2,29	2,2963
	3,074	3,1588
	2,227	2,2056
Y−O2 x 2	2,451	2,4744
	2,269	2,2861
	3,451	3,4858
	2,619	2,6487
B−O1 x 2	1,9397	1,9753
B−O2 x 2	1,977	1,9959
	1,957	1,9799
B−O1−B	146,06	143,98
B−O2−Bx 2	146,27	146,82

The lattice cell parameters, temperature factors and *R*-factors are given in Table 1, and selected distances and angles in the structure of these two perovskites is given in Table 2. $YCo_{0.5}Cr_{0.5}O_3$ has stable perovskite structure. The substitution of bigger Cr^{3+} with smaller Co^{3+} ion decreases the unit cell parameters, cell-volumes and the pseudo-parameter *a*. The distortion in $YCrO_3$ is mainly due to the octahedral tilting (Fig. 1). Substitution of Cr with Co influences change in parameters ratio *c*/*a*. For $YCrO_3$ $a \approx c$ and for $YCo_{0.5}Cr_{0.5}O_3$ $a>c$.

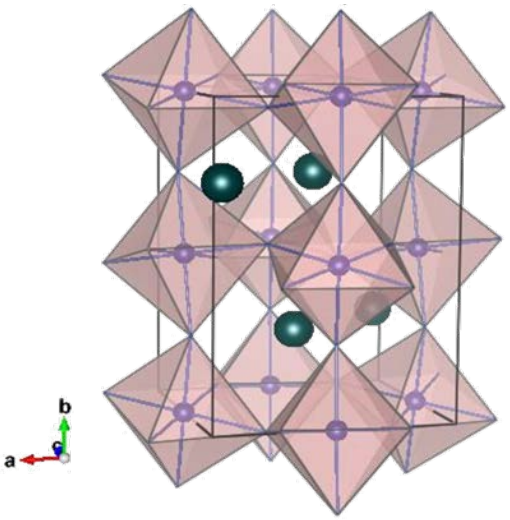

Fig. 1. The distortion of the BO_6 coordination octahedral in the orthorhombic perovskite strucure.

The sintered pellets were electroded by high purity ultrafine silver paste and then connected to the HP 4192A Impedance Analyzer for electrical characterization. We used *ac* impedance spectroscopy in order to avoid the electrode polarization. When applying the external electric field, electrically heterogeneous materials polarize and charge carriers move relatively easer through one of the phases than another one and they stack at grain boundaries. Charges build up at the interfaces and get polarized in the presence of the electric field,

depending on conductivities of the phases that build the ceramics.[3]. The real and imaginary part of the complex impedance were measured in series mode for determine bulk resistance and grain resistance of the sample. The amplitude of the applied *ac* electric field was 1V.

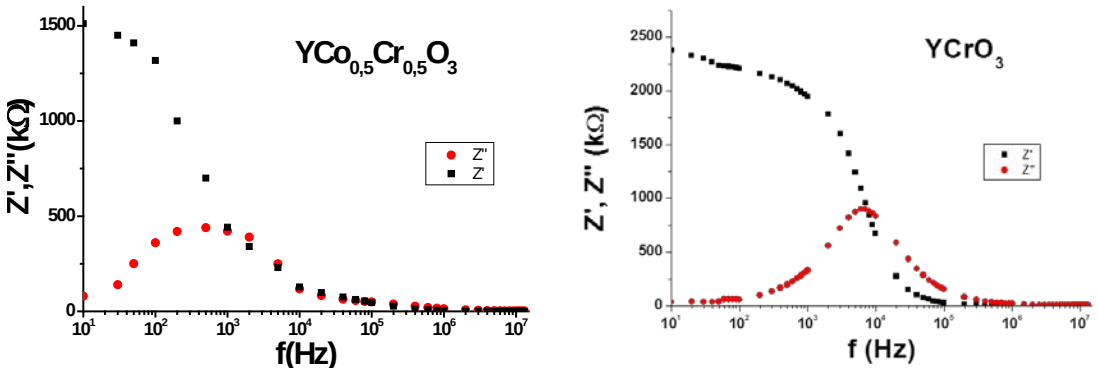

Fig. 2. Frequency dependence of real and imaginary part of $YCrO_3$ (a) and $YCr_{0,5}Co_{0,5}O_3$ (b) at 339 K.

Figure 2.a. and b. represents the frequency dependence of *Z'* and *Z"* of $YCrO_3$ and $YCo_{0.5}Cr_{0.5}O_3$ respectively. *Z'* decreases with increase in frequency for both samples implying relaxation process in the structures. The value of *Z'* is higher and *Z"* lower for $YCrO_3$ than for $YCo_{0.5}Cr_{0.5}O_3$, i.e. the conductivity is lower, because of the bigger radius of Cr. The presence of Co in the structures shifts the *Z"* peak towards lower frequencies increasing the relaxation times.

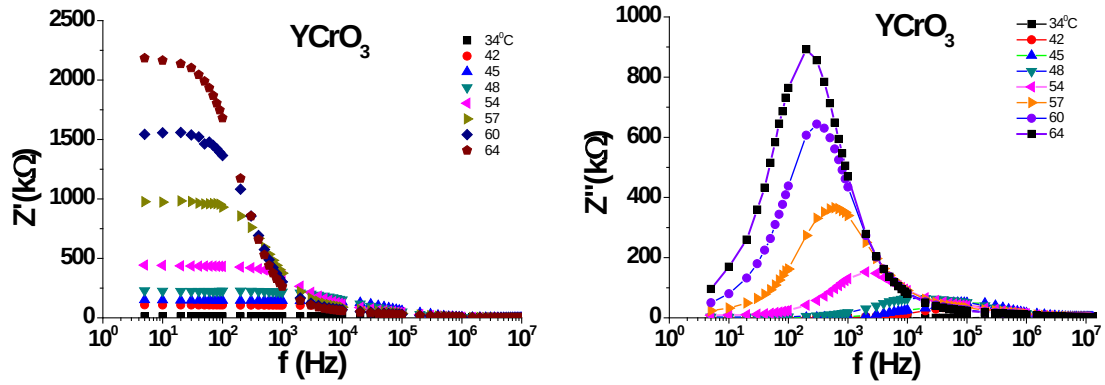

Fig. 3: Frequency dependence of *Z'* and *Z"* for $YCrO_3$ at different temperatures.

Figures 3 and 4 show the frequency dependence of *Z'* and *Z"* of $YCrO_3$ and $YCo_{0.5}Cr_{0.5}O_3$ respectively for different temperatures. Increasing of *Z'* and *Z"* and decreasing of conductivity at low frequencies with increasing temperature reveals positive temperature coefficient of resistance, i.e. metallic behavior of the samples. Release of the space charge is defined above 1MHz when all *Z'* values merge. *Z"* peak, centered at the dispersion region of *Z'*, shifts to lower frequencies with increasing temperature due to change in relaxation in the sample. A symmetric broadening of the peaks with the increase of temperature suggests the presence of temperature-dependent relaxation process of the materials.

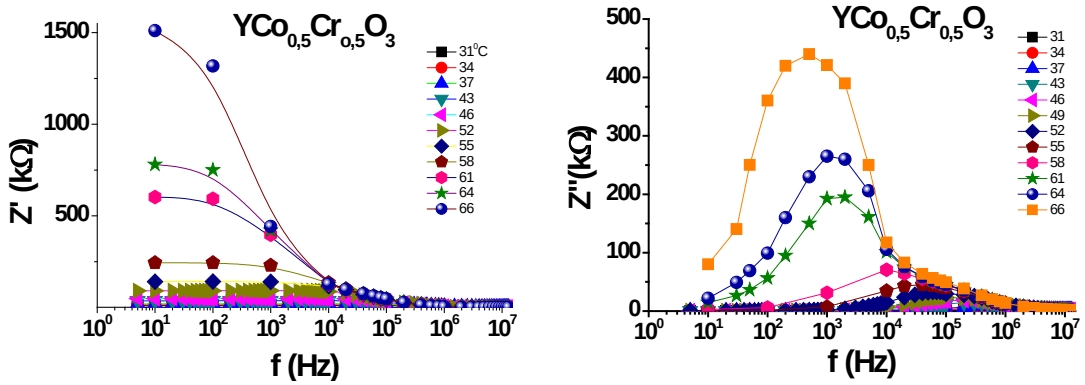

Fig. 4: Frequency dependence of *Z'* and *Z"* for $YCo_{0.5}Cr_{0.5}O_3$ at different temperatures.

The relaxation time $\tau_m = 1/\omega_m$ is determined for the position of maximum of *Z"*, where ω_m is angular frequency corresponding to this maximum. Calculated values of relaxation times for temperature interval 301– 337 K from the *Z"* versus log *f* plots are given in TABLE 3 for $YCrO_3$ and TABLE 4 for $YCo_{0.5}Cr_{0.5}O_3$. The value of relaxation times is increasing with increasing temperature which indicates conductor behavior of the structures, more pronounced for $YCrO_3$.[5] The most probable relaxation times within the investigated temperature range, follow the Arrhenius law given by:

$$\tau_m = \tau_0 \exp\left(\frac{E_a}{kT}\right), \tag{5}$$

where τ_0 is the pre-exponential factor, E_a is the activation energy of the possible process, *k* is Boltzmann constant and *T* is absolute temperature. From the linear least squares fit we observed two different slopes with obtained activation energies E_a of 0,949eV and 3,003eV for $YCo_{0,5}Cr_{0,5}O_3$ for temperature region 301-325 K and 325-337 K, and only one slope for whole temperature range with E_a= 2,73eV for $YCrO_3$.

Figure 5 represents the so-called Nyquist plot (*Z" vs Z'*) at different temperatures for $YCrO_3$. Here we can separate the grain effect at high frequencies from the grain boundary effect at lower frequencies. The presence of surface (electrode) polarization at low frequencies is not given on the graph. The last one is highly capacitive phenomenon, characterized by larger relaxation times than the polarization mechanism in the bulk. The results usually appear in two separate semicircles, one representing the bulk effect at high frequencies and the other surface effect at low frequency range. The sharp increase of the impedance with temperature, which is connected to the reducing of conductivity, confirms the conductive behavior of the material. Both grain and grain-boundary contribution represented with two overlapping arcs, are comparable in the material at lower temperatures. It is known [6] that, in electroceramics, if the pore size is greater than 1 μm, it would lead to the overlapping of the semicircles. With the increase of the temperature the grain boundary contribution increases rapidly and overcomes the grain effect. Single grain boundaries are insulating and with temperature increase they become dominant. The semicircle due to resistance within the grains of the materials becomes small

related to other arc due to the partial or complete blocking of charge carriers at grain boundaries. The electrical behavior of the structures can be described by RC equivalent circuits, one for the grain contribution and the other for grain boundary contribution.

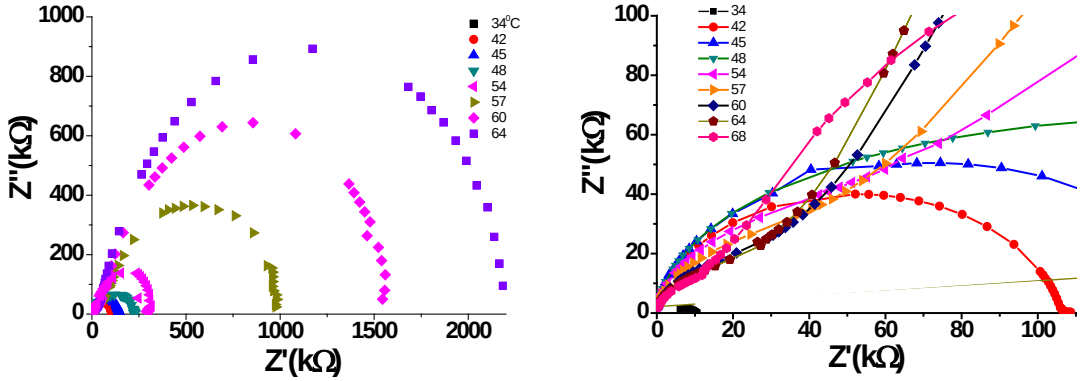

Fig. 5: a) Nyquist plot for $YCrO_3$ for various temperatures with dominant grain boundary effect. b) High frequency end of the plot showing the bulk processes in the structure.

The values of grain-boundary resistance are extracted from the intercept of the low frequency semicircle with the real axis and reveal that the rate of decrease of grain-boundary conductivity is different in different regions, which means different activation energies involved in different temperatures regions for the conductivity due to grain-boundary.[7] The grain-boundary resistance (R_{gb}) values are given in TABLE 4. The next graph, Fig.6, shows *Z' vs Z"* plot for $YCo_{0.5}Cr_{0.}5O_3$. The results are similar as for $YCrO_3$ with lower values of resistance. The presence of at least two depressed semicircles in the plot reveal non-Debye behavior with possible two relaxation processes for both structures. Intersection of the semicircle with the real axis shifts away from the origin with increase in temperature and the frequency of the intersection with real axis also increase with temperature.

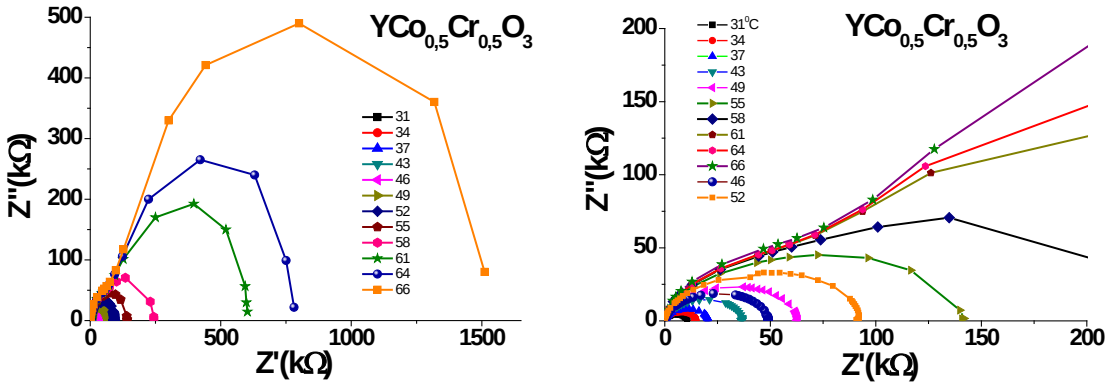

Fig. 6: a) Nyquist plot for $YCo_{0,5}Cr_{0,5}O_3$ for various temperatures with dominant grain boundary effect. b) High frequency end of the plot showing the bulk processes in the structure.

Table 3. Calculated values of grain boundary resistance, relaxation time and capacitance of $YCrO_3$.

T (K)	307	315	318	321	324	327	330	333	337
R_{gb} (kΩ)	10,5	108,6	146,6	229,9	264	441	977	1556	2184
τ (10^{-6}s)	0,177	1,59	2, 59	7,59	22,7	79,6	265	531	796
C (10^{-11}F)	0,686	1,465	1,551	3,463	8,616	18,053	27,164	34,112	36,455

Table 4. Calculated values of R_{gb}, relaxation time and capacitance of $YCo_{0,5}Cr_{0,5}O_3$.

T (K)	304	307	310	316	319	321	325	328	331	334	337
R_{gb} (kΩ)	10,4	14,1	19,7	36,1	48,9	62,5	90,9	140,8	243,8	593,4	750,2
τ (10^{-6}s)	0,027	0,027	0,318	0,796	0,796	1,59	1,99	3,98	15,9	31,8	79,6
C (10^{-11}F)	2,185	1,615	1,617	2,205	1,627	2,548	2,189	2,827	6,529	5,367	10,61

The *ac* conductivity for $YCrO_3$ and $YCo_{0,5}Cr_{0,5}O_3$ perovskites was calculated from measured real and imaginary parts of the impedance data and pellet dimensions. Figure 7 gives comparison between conductivities of two structures at 301 K showing higher values for $YCo_{0,5}Cr_{0,5}O_3$ confirming the results from the impedance measurements. We observe characteristic behavior of conductivity spectra, i.e. for low frequencies σ_{dc} is dominant and at higher frequencies conductivity increases with increasing frequency. The slope of the conductivity for high frequencies is lower for $YCo_{0.5}Cr_{0.5}O_3$ and the dispersion starts at higher frequencies compared to $YCrO_3$.

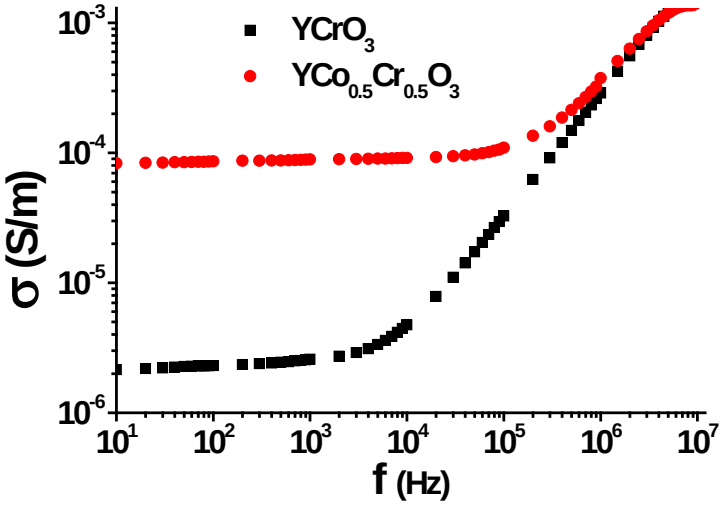

Fig. 7: Comparison of frequency dependent conductivity for both structures at 301K.

Conductivity obeys the Jonscher's power law for whole temperature region investigated:

$$\sigma = \sigma_{dc} + A\omega^n \quad , \quad 0 < n < 1 \tag{6}$$

A plateau is significant at lower temperatures and disappears with increase of temperature (Fig.7), while σ_{ac} is proportional to the increase of frequency, obeying power law. The frequency at which the dispersion region starts from the *dc* conductivity plateau can be defined as the characteristic frequency (f_p) where the relaxation effects of the ions occur. This

characteristic frequency is termed as hopping rate (f_p) or cross over frequency and it occurs at $\sigma_{fp}=2\sigma_0$. The relation between the *dc* conductivity and the hopping rate is given by $\sigma_{fp} = k\,2\pi f_p$ where k is the empirical constant, which depends on the concentration of mobile ions and type of the conduction mechanism.

Figure 8 and Figure 9 give the frequency dependent conductivity of $YCrO_3$ and $YCo_{0.5}Cr_{0.5}O_3$ respectively for various temperatures. Observed decreasing σ_{dc} with increasing temperature confirmed the conduction behavior for both $YCrO_3$ and $YCo_{0.5}Cr_{0.5}O_3$. The values of σ_{dc} obey Arrhenius plot from which we calculated activation energies for conducting process:

$$\sigma = \sigma_0 \exp\left(-\frac{E_a}{kT}\right) \tag{7}$$

The activation energy for *dc* conductivity is found to be 0,934 eV for $YCrO_3$ and 0,867 eV for $YCo_{0.5}Cr_{0.5}O_3$ until 325 K. With increasing temperature above 325 K E_a goes to 1,106 eV for $YCrO_3$ and 2,018eV for $YCo_{0.5}Cr_{0.5}O_3$. The behavior of two samples is similar, but with higher values of *dc* conductivity for $YCo_{0.5}Cr_{0.5}O_3$.

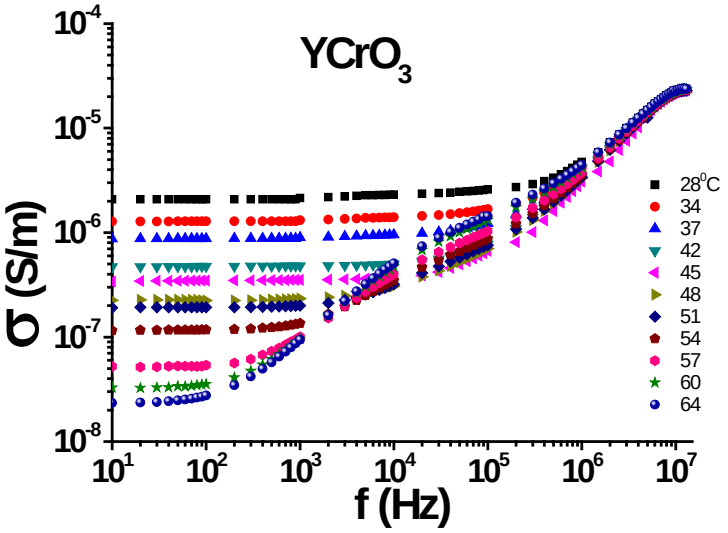

Fig. 8: Frequency dependent conductivity of $YCrO_3$ for various temperatures.

We investigated *ac* conductivity behavior with temperature for various frequencies and observed strong dependence at low frequencies and almost temperature independent conductivity at high frequencies (the region where ions are not capable of responding the alteration of external electric field).The dispersion region increases with increase in temperature, whereas characteristic frequency f_p shifts towards the low frequencies. The conductivity is changing its behavior with increasing frequency and different slopes are observed at different ranges of frequency. We observe two regions predominant with different conduction mechanisms. At the low temperature region, the conduction is presumably predominant by the extrinsic impurity conduction with a very similar activation energy, whereas the conduction at the high temperature range is likely predominant by intrinsic defects [8].

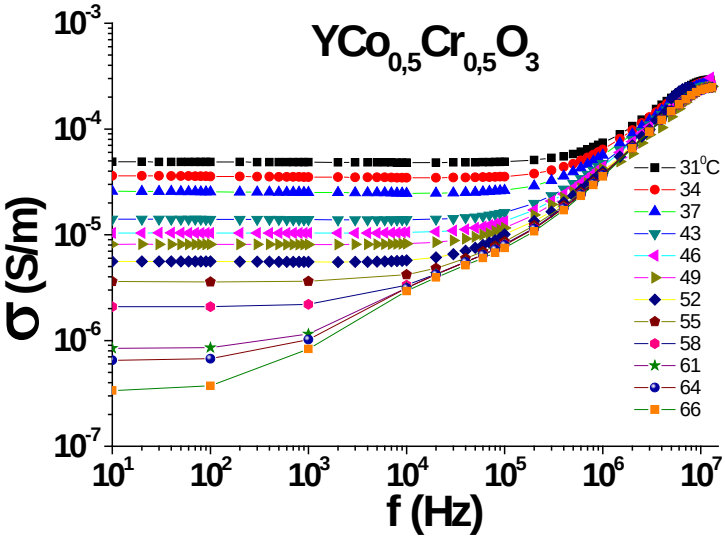

Fig. 9: Frequency dependent conductivity of $YCo_{0,5}Cr_{0,5}O_3$ for various temperatures

The activation energy for f_p was estimated to 1,007eV and 0,975eV until 325K and 2,889eV and 3,5eV over 325K for $YCrO_3$ and $YCo_{0.5}Cr_{0.5}O_3$ respectively. Compared to the activation energies for *dc* conductivity they are similar for low temperature measurements, where both grain and grain boundary effect are equally presented, and vary a great deal at higher temperatures where grain boundary effect becomes dominant.

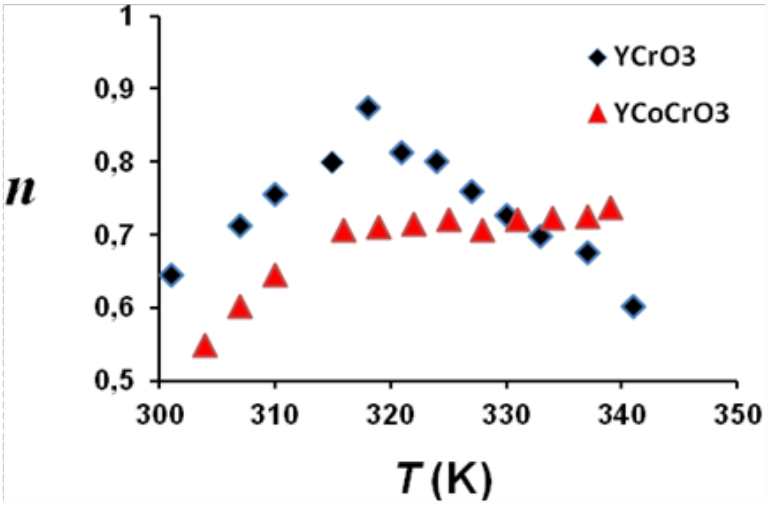

Fig. 10: Variation of exponent *n* from power law with temperature.

The results of fitting the *ac* conductivity to Jonscher power law show changes of conductivity behavior with increasing temperature. The observed enhancement of the exponent *n* with increasing temperature until 325 K for both samples with slightly higher values of *n* for $YCrO_3$, i.e. increasing *ac* conductivity is attributed to the existing oxygen vacancies and increasing concentration of ions, impurities which are more thermally activated by heating at lower temperatures. The difference in the behavior is observed for temperatures over 325 K

where *n* is decreasing for $YCrO_3$ while for $YCo_{0.5}Cr_{0.5}O_3$ remains almost constant (Fig.10). This explains the change of the slope of conductivity in $YCrO_3$ because of higher concentration of grain boundaries and constant slope in $YCo_{0.5}Cr_{0.5}O_3$. This confirms the conclusion from the X-ray diffraction analysis for more stable crystal structure of $YCo_{0.5}Cr_{0.5}O_3$ and distortion in $YCrO_3$ due to the octahedral tilting.

3. CONCLUSIONS

In this article we investigated the electrical properties of two types of perovskites $YCrO_3$ and $YCo_{0.5}Cr_{0.5}O_3$. They were prepared by solution combustion method and additionally heated at 800^0C for 4 hours and after submitted to X-ray diffraction analysis their structure was defined as orthorhombic space group *Pnma* with four formula units per unit cell. $YCo_{0.5}Cr_{0.5}O_3$ has stable perovskite structure, while distortion in $YCrO_3$ is mainly due to the octahedral tilting.

Influence of the substitution of Cr with Co on the impedance and conductivity is investigated for frequency range 10-10^7 Hz and temperature range 301-339 K using complex impedance spectroscopy technique involving *ac* electric field. The results reveal increase of *Z'* and *Z"* and decrease of conductivity with temperature confirming metallic behavior of the structures. From the Nyquist plot we observed two relaxation processes for both samples, i.e. both grain and grain boundary contribution are present in the relaxation process. Their behavior is similar, but the impedance is lower i.e., conductivity is higher for $YCo_{0.5}Cr_{0.5}O_3$ confirming better structure with less grain boundary defects which influence its electrical behavior. The values of R_{gb} for different temperatures were extracted from the plot and they confirm the previous conclusion since $YCo_{0.5}Cr_{0.5}O_3$ has lower values of resistance than $YCrO_3$. The broadening of *Z"* with increase of temperature suggests temperature dependent relaxation process. The values of activation energies calculated from the slope $\ln\sigma$ versus 1000/T are similar to those obtained from Arrhenius plot of relaxation times. The *ac* conductivity behavior is analyzed using Jonscher's power law $\sigma = A\omega^n$. Both structures have similar behavior at low temperatures with lower value of *n* for $YCo_{0.5}Cr_{0.5}O_3$. The influence of Co in the structure is observed in the high frequency region where the value of *n* is almost constant, while for $YCrO_3$ it is decreasing.

REFERENCES

[1] Principles of Electronic Ceramics, L. L. Hench and L. K. West, John Wiley & Sons,Inc., (1990), pp 244-247.

[2] Observation of local non-centrosymmetry in weakly bifferoic $YCrO_3$, K.Ramesha, A.Llobet, Th. Proffen, C. R. Serrao and C. N. R, Rao, *J.Phys: Condens. Matter* **19,** 102202 (2007)

[3] Effect of sintering on microstructure and dielectric response in $YCrO_3$ nanoceramic, J.Bahadur, D.Sen, S Mazumder, V.K. Aswal, V. Bedekar, R. Shukla and A. K. Tyagi, pp.959-963,*Pramana- Journal of Physics*, **71**, 5 (2008)

[4] Formation, powder characterization and sintering of $YCrO_3$ prepared by sol-gel technique using hydrazine, T.Tachiwaki, Y.Kunifusa, M. Yoshinaka, K.Hirota, O.Yamaguchi, International *Journal of Inorganic Materials* **3**, 107-111 (2001)

[5] Crystallographic phases, phase transitions and barrier layer formation in $(1-\boldsymbol{x})[Pb(Fe_{1/2}Nb_{1/2})O_3]-\boldsymbol{x}PbTiO_3$, Singh S P, Singh A K, Pandey (2003) *J. Mater. Res.* **18** (11) 2677-2687

[6] Densification of Yttria-stabilized zirconia impedance spectroscopy analysys, M. C. Steil, F . Thevenot and M. Kleitz, *J. Electrochem.Soc.* **144** (3) (1997) 390

[7] Impedance spectroscopy analysis of double perovskite Ho_2NiTiO_6, Dev K. Mahato, A. Dutta, T. P. Sinha, *J. Mater. Sci.* (2010) **45**:6757–6762

[8] Dielectric properties of layered perovskite $S_{1-x}A_xBi_2Nb_2O_9$ ferroelectrics. A=La,Ca and x=0,0.1., M. J. Forbess, S. Seraji, Y. Wu, C. P. Nguyen, and G. Z. Caoa, *Appl. Phys. Lett.*, **76** (20)